Silicotungstic Acid Based Carbon Supported Noble Metal Electrodes for Energy Conversion Application

ARTICLE *in* THE JOURNAL OF PHYSICAL CHEMISTRY C · JULY 2009

Impact Factor: 4.77 · DOI: 10.1021/jp8100514

3 AUTHORS, INCLUDING:

Satyananda Kishore Pilli
Colorado School of Mines
16 PUBLICATIONS **341** CITATIONS
SEE PROFILE

Balasubramanian Viswanathan
Indian Institute of Technology Madras
454 PUBLICATIONS **6,394** CITATIONS
SEE PROFILE

Silicotungstic Acid Based Carbon Supported Noble Metal Electrodes for Energy Conversion Application

P. Satyananda Kishore, B. Viswanathan,* and T. K. Varadarajan

National Centre for Catalysis Research, Indian Institute of Technology Madras, Chennai 600036, India

Received: August 13, 2008; Revised Manuscript Received: April 28, 2009

In this paper, carbon supported noble metal nanoparticles synthesized by using Keggin type polyoxometalate (POM), silicotungstic acid (STA), were effectively utilized as electrodes in an effort to improve the efficiency of electrochemical energy conversion processes related to direct methanol fuel cells. The excellent electron transfer and strong adsorption abilities of STA have been well exploited for the reduction of metal ions as well as the modification of carbon support to form Pt and Pt−Ru metal nanoparticles supported on carbon nanostructure composites (Pt/STA-C and Pt−Ru/STA-C) under microwave irradiation. Transmission electron microscopy results indicated that well-dispersed metal nanoparticles were formed on the carbon support. The electrocatalytic properties of Pt/STA-C and Pt−Ru/STA-C were analyzed by cyclic voltammetry and chronoamperometry through the methanol oxidation reaction for fuel cell applications. As compared with the commercial Pt−Ru/C (Johnson Matthey) and Pt/C and Pt−Ru/C electrocatalysts prepared by using the common hydrogen reduction method, the STA containing Pt/STA-C and Pt−Ru/STA-C synthesized by the method developed in this work exhibited lower onset potential, high activity with enhanced stability, and better tolerance toward poisoning by CO for the methanol oxidation reaction.

Introduction

In modern society there is an enormous demand for energy. Hence, the development of new energy sources and improvement of energy efficiency in conversion has become important. Electrochemical energy production is under serious consideration as an alternative energy/power source as it is designed to be more sustainable and environmentally friendly.[1] The development of new materials that can solve the challenging problems in the areas of energy conversion is of paramount importance in the quest to improve the efficiency of these devices. Supported metal nanoparticles based electrodes have shown improved activity in electrochemical energy conversion processes.[2] However, there is a need for further modification of these materials to overcome some issues.

In electrochemical energy conversion devices such as direct methanol fuel cells (DMFCs), carbon-supported noble metal nanoparticles remain the choice of electrocatalyst due to their high electrocatalytic activities for both the oxidation of methanol at anode and the reduction of oxygen at cathode.[3−5] However, high cost of the precious metal platinum for the electrodes, sluggish kinetics, and poor methanol oxidation at anode due to poisoning caused by CO like species remained the main challenges, and hence, effective commercialization of fuel cell is lagging behind.[6−8] Effective anode catalysts are required for not only accelerating dehydrogenation reaction but also improving the tolerance toward CO poisoning. Several strategies were adopted to modify the Pt surface in order to improve its catalytic activity and sensitivity regarding poisoning species. To promote the release of CO species from Pt and spare more available surface for methanol electro-oxidation, oxygen containing species adjacent to the Pt sites are required. Due to the lower potential for producing oxygen-containing species on Ru, alloys of platinum with Ru or oxophilic metals have been explored as CO tolerant catalysts based on bifunctional mechanism.[9−13] Alternatively, Pt nanoparticles have been immobilized on large surface area inorganic oxide nanomaterials.[14−18] Supporting Pt nanoparticles on metal oxides also facilitate mutual metal−support interactions and dispersion of catalytic centers. This provides unimpeded charge distribution and good overall stability to Pt nanoparticles.

Considering the beneficial effects of nanomaterials of metal oxides and noble metal nanoparticles in improving the activities of energy conversion processes, it is of great significance to develop an innovative strategy using a single reagent through which a dual role (formation of well-dispersed oxide environment around metal nanoparticles and effective promotion of electrochemical energy conversion processes) can be performed. Therefore, in the present study an innovative strategy is employed for the development of efficient materials for energy conversion (anode electrocatalyst for fuel cells) using tungsten based Keggin type polyoxometalate (POM), silicotungstic acid (STA). Apart from providing ultimate dispersion of oxide environment,[19] fast electron transfer capability and high proton conducting ability makes STA as an attractive species for electrochemical applications. It ensures enhanced availability and mobility of the protons as well as electrons at the electrocatalytic interfaces.[20−22] In this regard, we explored a facile, efficient and simple route to obtain carbon (Vulcan XC-72 or C) supported metal nanoparticles composites containing STA (Pt/STA-C and Pt−Ru/STA-C) by exploiting STA's excellent electron transfer as well as adsorption capabilities. In order to compare the efficiency of the as synthesized composites, STA free (Pt/C and Pt−Ru/C) composites were prepared using common hydrogen reduction method. The Pt/STA-C and Pt−Ru/STA-C hybrid materials exhibited high electrocatalytic activity for methanol oxidation in terms of activity and stability compared to STA free Pt/C and Pt−Ru/C and commercially available Johnson Matthey 20% Pt−Ru/C catalyst. Over all the developed nanocomposites (Pt/STA-C and Pt−Ru/STA-C)

* Corresponding author. E-mail: bvnathan@iitm.ac.in. Fax: +91 44 2257 4202.

10.1021/jp8100514 CCC: $40.75
Published on Web 06/25/2009

SCHEME 1: Schematic Representation of the Preparation of Carbon Supported Pt Nanoparticles by STA

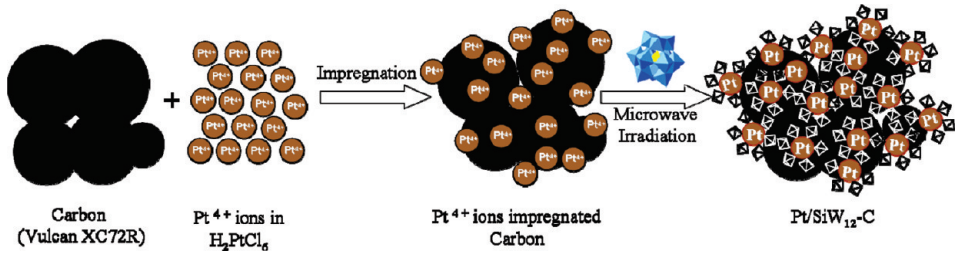

containing STA are multifunctional in terms of promoting the energy conversion process. This research may also open a new approach for designing other hybrid materials with multi functionality for various electrochemical processes.

Experimental Section

Materials. Silicotungstic acid, hexachloroplatinic acid and ruthenium trichloride were procured from Sigma-Aldrich and used as received. Carbon Black (Vulcan XC-72R, Cabot) with specific surface area (BET) of 250 $m^2 g^{-1}$ was used as the carbon support for all of the catalysts. Double distilled water was used for the preparation of all the aqueous solutions. High-purity hydrogen and nitrogen were used in the experiments. A microwave oven operating at low power setting (frequency of 2450 MHz, maximum power 700 W) was used for microwave irradiation.

Preparation of Reduced Silicotungstic Acid (STA). An aqueous solution of STA (10 mM) was treated with 2-fold excess of Zn metal powder. The solution turned blue indicating the formation of "heteropoly blue" (reduced form of STA). It was then filtered and the obtained filtrate was used as reducing agent for the reduction of metal ions.

Preparation of Pt/STA-C and Pt−Ru/STA-C by STA Reduction Method. A schematic illustration of the preparation of Pt/STA-C composite is given in Scheme 1. The carbon source was impregnated with hexachloroplatinic acid to get the Pt metal ions loaded carbon. In order to reduce and stabilize the metal ions on the carbon support, reduced STA (blue colored species) was added and simultaneously irradiated with microwave radiation. The blue color of the solution changed to colorless indicating the oxidation of STA. For comparison, the Pt or Pt−Ru loadings in all the composites were done at the nominal Pt level in the commercial catalyst, i.e., 20 wt % of Pt or Pt−Ru. The typical procedure involved the following steps. Specific amounts of hexachloroplatinic acid (10 mM) or hexachloroplatinic acid (10 mM) and ruthenium(III) chloride hydrate (10 mM) were loaded on carbon to get 20 wt % metal loading by conventional impregnation method. The composition of Pt and Ru was fixed to produce a final atomic ratio of 1:1 in the preparation of all Pt−Ru based composite catalysts. The mixture was magnetically stirred for 3 h at room temperature and then evaporated to dryness at 80 °C. Reduced STA (10 mM) was added to the impregnated material, followed by microwave irradiation for 90 s. The color of the reduced STA was changed from blue to colorless indicating the oxidation of STA, ensured the electron transfer from STA to metal ions. The final solid products of 20% Pt/STA-C and 20% Pt−Ru/STA-C were obtained by centrifugation, washed with water and then dried in vacuum at 70 °C for 8 h.

Preparations of STA Free 20% Pt/C and 20% Pt−Ru/C by Hydrogen Reduction Method. For comparison, a second set of catalysts, 20% Pt/C and 20% Pt−Ru/C were prepared by impregnation method with similar composition as mentioned above. The resultant material was then introduced into a tubular furnace and reduced under flowing H_2 gas at 350 °C for 3 h.

Instrumentation. The transmission electron micrographs (TEM) and energy-dispersive X- ray spectroscopy analysis (EDAX) were performed on CM12/STEM microscope operating at a 100 kV accelerating voltage. HRTEM micrographs were recorded using JEOL-3010 transmission electron microscope operating at 300 kV. To obtain TEM images, the as synthesized electrocatalysts dispersed in ethanol solution were coated on a Cu-carbon grid. UV−visible spectra were recorded on Cary 5E UV−vis-NIR spectrometer. Powder X-ray diffraction patterns were recorded using a SHIMADZU XD-D1 diffractometer using Cu Kα radiation (λ = 1.5418 Å). FT-IR investigations were performed on Perkin-Elmer 1760 in the region 1100−400 cm^{-1} by using KBr pellet mode.

Electrochemical Measurements. A conventional, three-electrode cell consisting of glassy carbon (GC) with an area 0.07 cm^2 as the working electrode, Pt foil counter electrode and Ag/AgCl (Saturated by KCl solution) electrodes as a reference electrode were employed for all the electrochemical measurements. The GC electrode was polished to a mirror finish with 0.05 μm alumina suspension, washed with water before each experiment, which served as an underlying substrate of the working electrode. The working electrode for the electrochemical measurements was fabricated by dispersing 10 mg of the electrode material in 300 μL of distilled water and the dispersion was then sonicated for 20 min. A quantity of 10 μL of this ink was pipetted out on the top surface of the GC using a micropipet and dried in a convection oven at 80 °C for about 10 min to obtain a thin active layer. Finally the resulting film was covered with 5 μL of Nafion to bind the particles on the substrate and dried at room temperature.

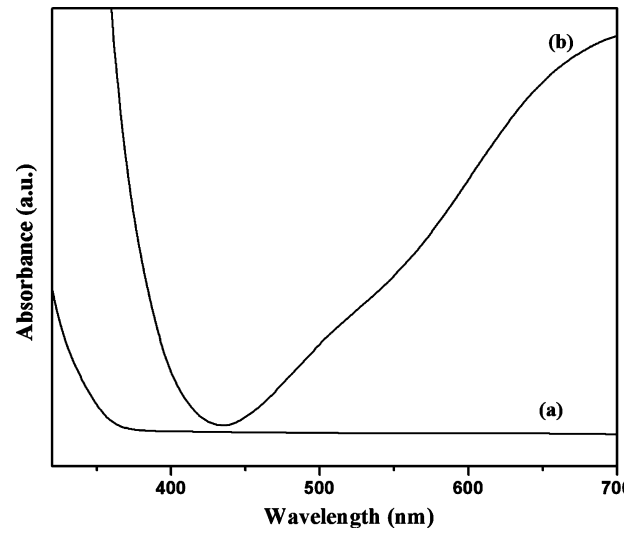

Figure 1. UV−vis spectra of (a) pure STA and (b) reduced STA.

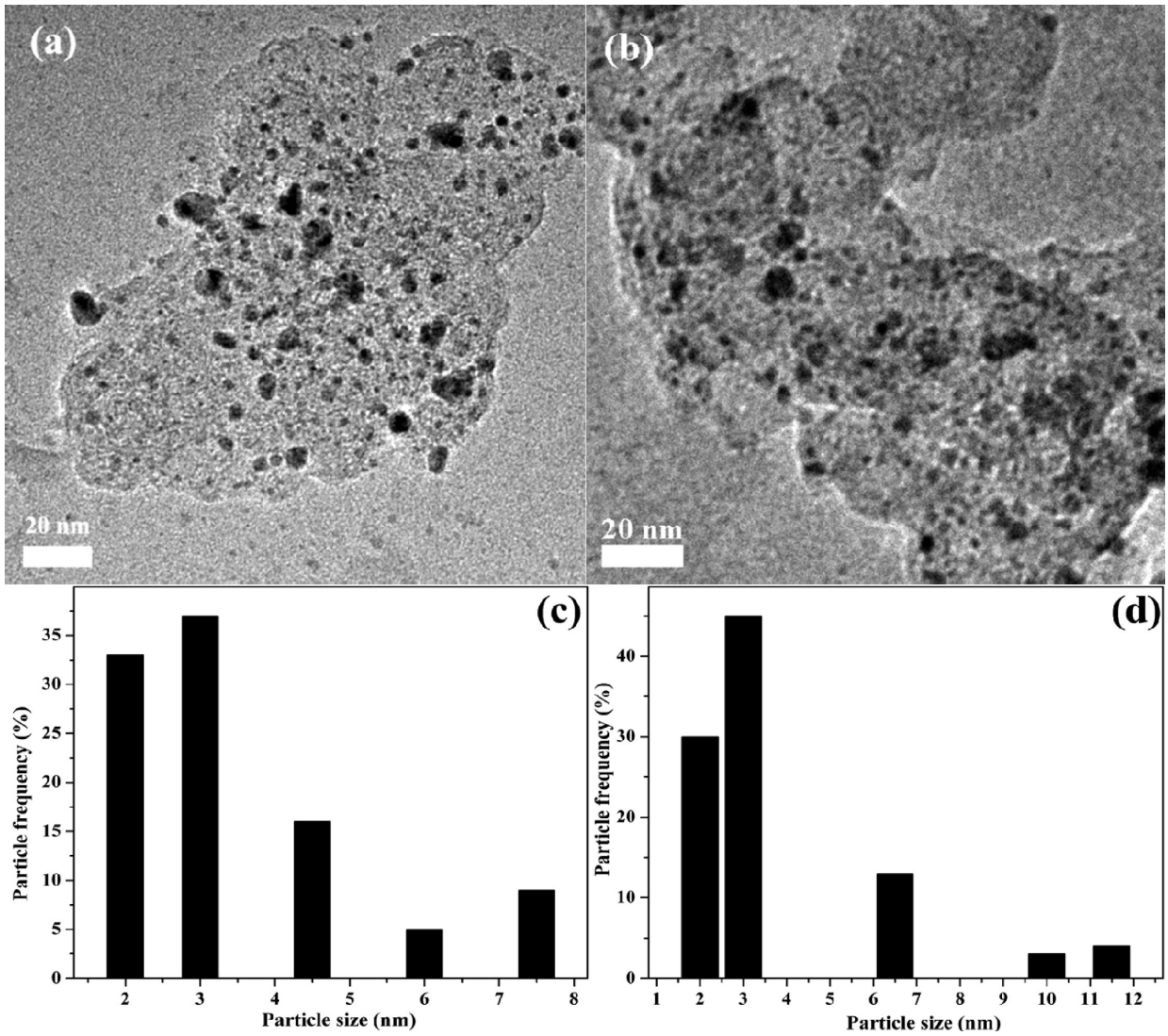

Figure 2. TEM images of (a) Pt/STA-C and (b) Pt- Ru/STA-C. Size distribution of particles in Pt/STA-C (c) and Pt−Ru/STA-C (d).

The methanol oxidation studies of Pt and Pt−Ru based composites (Pt/STA-C, Pt−Ru/STA-C, Pt/C, Pt−Ru/C, and commercial catalyst Pt−Ru/C (J.M)) catalysts were performed using a BAS Epsilon potentiostat. The activity of the electrodes were determined using cyclic voltammetric (CV) and chronoamperometric experiments in 1 M H_2SO_4 solution in the presence of 1.0 M CH_3OH. All of the solutions were prepared by using ultrapure water (Millipore, 18 MΩ). The electrolyte solution was purged with high pure nitrogen for 30 min prior to a series of voltammetric experiments.

Results and Discussion

Characterization of the Reduced STA. The reduction of STA was followed by observing changes in the optical spectra of the STA in aqueous solutions as shown in Figure 1. The aqueous solution containing oxidized form of STA was colorless (W metal in d^0 state) and showed no absorbance in the range of 400−700 nm (Figure 1a). Whereas, the blue colored filtrate obtained from the mixture of STA and Zn metal powder, showed an absorption band at 700 nm (Figure 1b). The produced d^1 metal ion[23] of W was responsible for the d-d transition resulting in absorption in the visible region. This indicated the formation of reduced "heteropoly blue" of STA. The addition of reduced STA to Pt and Ru metal ions impregnated carbon under microwave irradiation led to a change in color of the solution from blue to colorless due to the oxidation of STA, indicating effective electron transfer from STA to metal ions. This electron transfer is feasible due to the relatively high reducing capacity of one equivalent reduced tungstate couple ($^{E^\circ}[SiW_{12}O_{40}]^{4-}/[SiW_{12}O_{40}]^{5-} = 0.057$ V vs NHE); (NHE = Normal Hydrogen Electrode) and favorable oxidizing capacity of Pt^{4+} ($^{E^\circ}PtCl_6^{2-}/Pt^0 = 0.725$ V vs NHE).

Physicochemical Characterization of the Electrocatalysts. To examine the immobilization of Pt or Pt−Ru nanoparticles on composites, transmission electron microscopy (TEM) measurements of the prepared catalysts were carried out. Figure 2 displays the representative TEM images and size distribution of catalysts Pt/STA-C and Pt−Ru/STA-C. As shown in panels a and b of Figure 2, the Pt and Pt−Ru nanoparticles of Pt/STA-C and Pt−Ru/STA-C are well dispersed on the carbon support and the particles are uniformly distributed without any aggregation. In addition, the Pt nanoparticles of Pt/STA-C composite exhibited a relatively narrow size distribution of 2−8 nm, with approximately more than 50% of them centered around 2−3 nm (Figure 2c). A statistical analysis of the TEM image showed that Pt nanoparticles have an average diameter of 3.4 nm, with a size distribution standard deviation of 1.6 nm in the Pt/STA-C composite. Pt−Ru nanoparticles in the Pt−Ru/STA-C

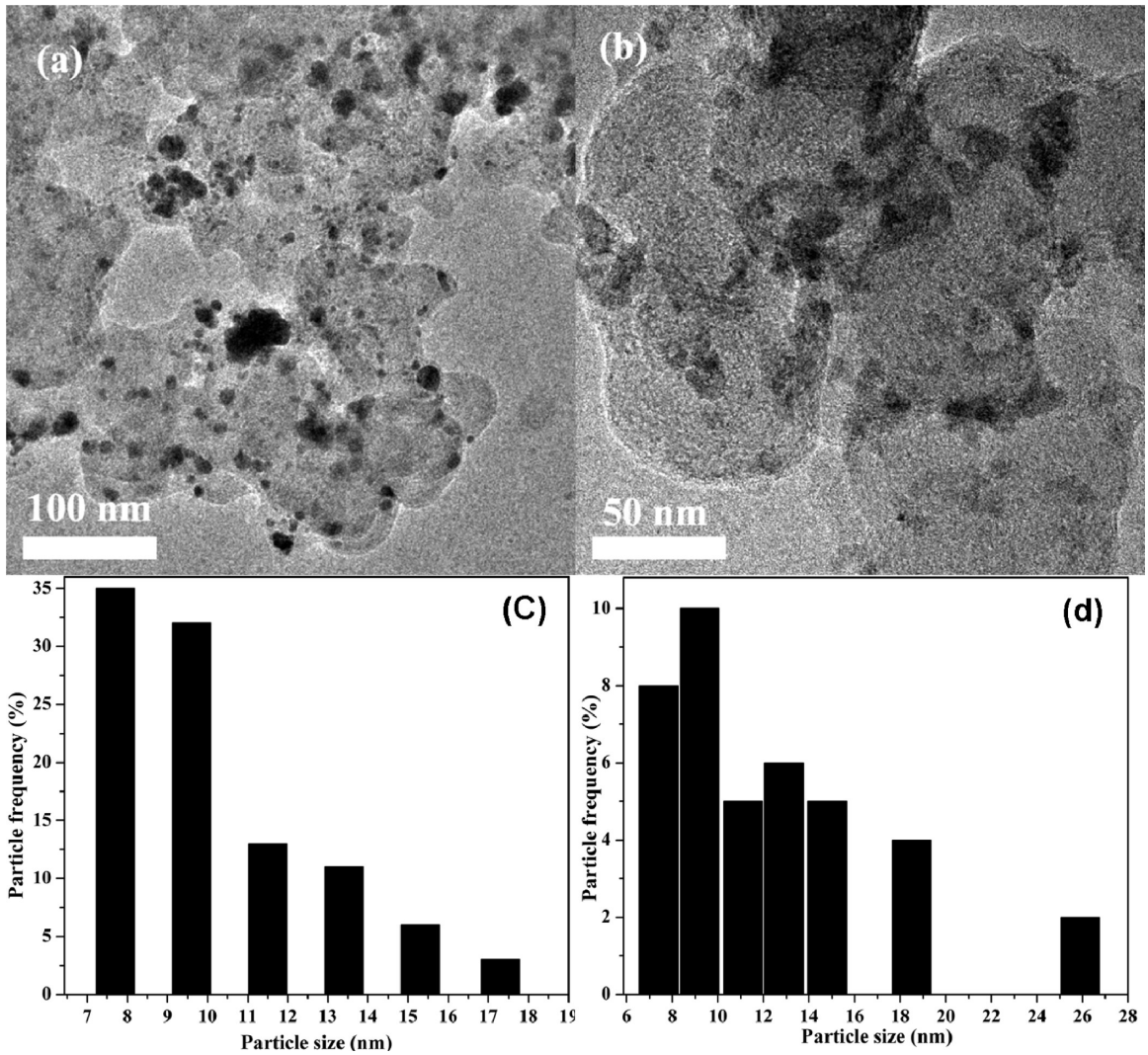

Figure 3. TEM images of (a) Pt/C and (b) Pt−Ru/C. Size distribution of particles in Pt/C (c) and Pt−Ru/C (d).

composite have an average diameter of 3.6 nm, with a size distribution standard deviation of 2.4 nm in Pt−Ru/STA-C composite. In comparison, a number of nanoparticles in Pt/C and Pt−Ru/C prepared by hydrogen reduction method appear to congregate, as shown in panels a and b of Figure 3, respectively. TEM image analyses and the particle size distribution revealed that Pt and Pt−Ru nanoparticles on carbon support (panels c and d of Figure 3) produced by the hydrogen reduction method resulted in larger particles with mean diameters of 10.2 and 16.5 nm respectively. Although the carbon support can inhibit the thermally driven Ostwald ripening of small Pt particles to some extent, the control of particle size and size distribution by this simple hydrogen reduction methodology is rather limited.[24] Hence, the Pt and Pt−Ru nanoparticles of Pt/STA-C and Pt−Ru/STA-C synthesized using STA reduction method is more efficient in terms of fabrication of particles with smaller size with better dispersion on the carbon support. This can be attributed to the repulsive interaction between the like-charged POMs (STAs) which have the ability to prevent the agglomeration of the metal nanoparticles.[25,26]

The detailed structure of the Pt and Pt−Ru nanoparticles dispersed on carbon in the Pt/STA-C and Pt−Ru/STA-C composites was further revealed by HRTEM analysis and the results were shown in Figure 4. From panels a and b of Figure 4, the formation of carbon nanobelts with highly dispersed Pt nanoparticles can be observed. The formed Pt nanoparticles have clear crystalline planes aligned along a specific direction with a *d* spacing of 2.27 Å (Figure 4c). Similarly, the lattice fringes of Pt−Ru nanoparticles are evident from HRTEM images of Pt−Ru/STA-C (Figure 4d). The formation of carbon nanosructures is possible because of the strong chemisorption of STA anions on carbon under microwave irradiation. STA has the ability to form electro-active adsorbate layer on metal surfaces such as platinum,[27] silver[28] and carbon surface[29] with high immobilization strength. A relatively short microwave irradiation (90 s) has driven STA to attach spontaneously to the carbon surface. The adsorbed polyanions provide static repulsion on carbon surface and allow the transformation into carbon nanostructures.[29] A similar effect was observed wherein, carbon nanostructures such as carbon nanotubes, nanobelts and nanoparticles,[30] quasi two-dimensional graphite sheets[31] were formed by the strong adsorption of various POMs on carbon surface under different energetic conditions.

The composites Pt/STA-C, Pt−Ru/STA-C and Ru/STA-C were also analyzed by EDX analysis (see Figure S1 in the Supporting Information). In addition to the metal and carbon peaks, the results showed the peaks due to Si, W, and O confirming the presence of STA. EDX analysis of 20% Pt−Ru/STA-C revealed that the atomic composition of Pt: Ru is 0.49: 0.51, which is close to 1:1 stoichiometry. SEM and EDAX of C, Pt, Si, W and O elements mapping (see Figure S2 in the Supporting Information) were carried out for the Pt/STA-C

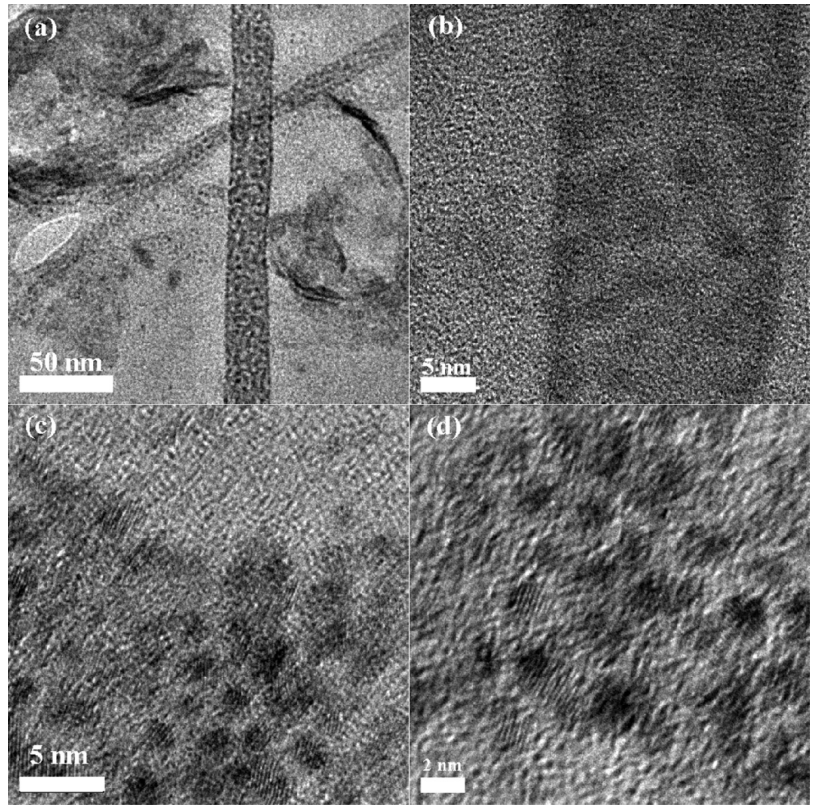

Figure 4. High Resolution TEM images of Pt/STA-C (a−c) and Pt−Ru/STA-C (d).

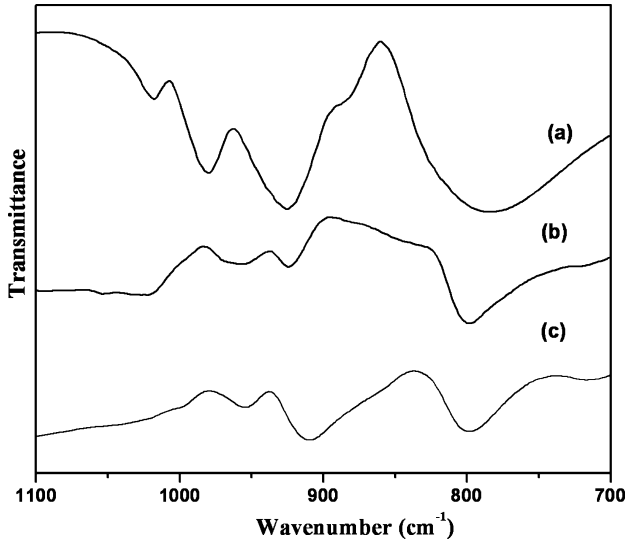

Figure 5. FTIR spectra of (a) pure STA, (b) Pt/STA-C, and (c) Pt−Ru/STA-C.

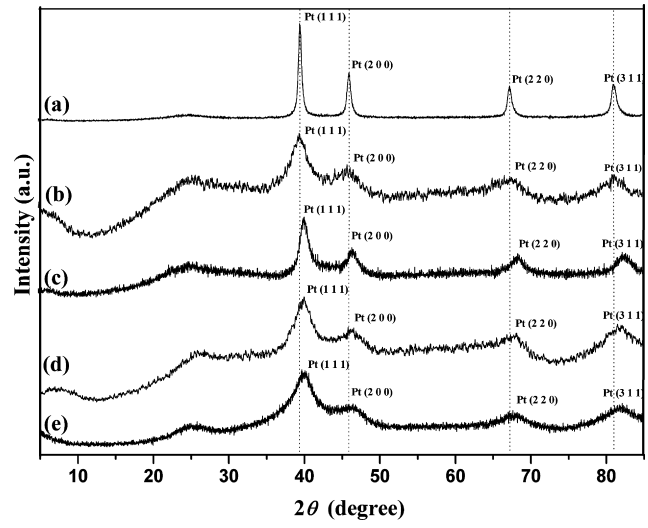

Figure 6. XRD patterns of (a) Pt/C, (b) Pt/STA-C, (c) Pt−Ru/C, (d) Pt−Ru/C (J. M), and (e) Pt−Ru/STA-C.

composite in order to observe the distribution of STA on the carbon support. The uniform distribution of Pt along with Si, W and O were observed, which further confirmed the presence of adsorbed STA around Pt nanoparticles.

To confirm the presence of STA and its chemisorption on the carbon surface in Pt/STA-C and Pt−Ru/STA-C composites, FT-IR (Figure 5b,c) measurements were carried out. For comparison, FT-IR response of pure STA is provided in Figure 5a, which exhibited four characteristic absorption bands at 1025, 980, 926, and 784 cm^{-1} ascribed to vibrations: ν_s(W−O), ν_{as}(W=O), ν_{as}(Si−O), and ν_{as}(W−O−W) respectively in the hydrated Keggin unit of STA.[32] The STA chemisorption in the Pt/STA-C and Pt−Ru/STA-C composites was evident from the presence of unique bands of the STA in FT-IR spectra (Figure 5b,c). Slight shift in the ν_{as}(Si−O) bands were observed due to the adsorption of STA on the carbon surface. The band due to external ν_{as}(W=O) is not obvious in these composites, inferring the strong interaction between carbon and STA due to chemisorption through the formation of W−O−C bond.

The as-prepared composites were also characterized by powder XRD, as shown in Figure 6. XRD is a bulk analysis that reveals the crystal structure, lattice constants and crystal orientation of the supported catalysts. According to previous reports, pure Pt has a face-centered cubic (fcc) crystal structure.[33] With the addition of Ru, which has a hexagonal close-packed (hcp) crystal structure, the diffraction peaks of the Pt−Ru will start to broaden and shift to higher 2θ values due to lattice

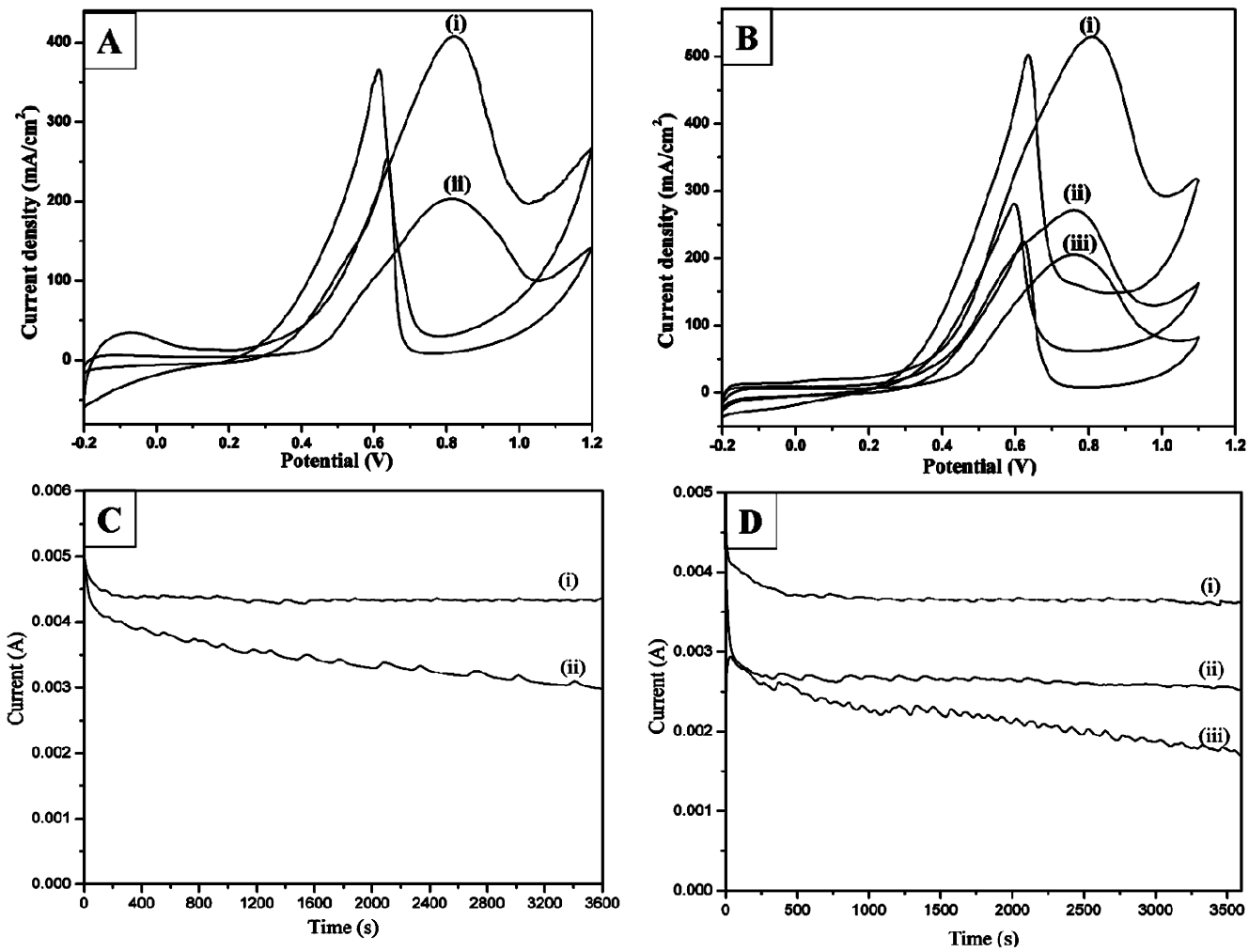

Figure 7. Cyclic voltammograms of (A) (i) Pt/STA-C and (ii) Pt/C; (B) (i) Pt- Ru/STA-C, (ii) Pt−Ru/C (J.M), and (iii) Pt−Ru/C in 1.0 M CH_3OH-1.0 M H_2SO_4 saturated by N_2 at a scan rate of 25 mV s^{-1}. Chronoamperometric responses of (C) (i) Pt/STA-C and (ii) Pt/C; (D) (i) Pt−Ru/STA-C, (ii) Pt−Ru/C (J.M) and (iii) Pt/ C in 1.0 M CH_3OH - 1.0 M H_2SO_4 saturated by N_2 at a constant potential of 0.5 V.

contraction.[34] Our results as shown in Figure 6, were very consistent with those literature reports for Pt and Pt−Ru. All the XRD responses Pt and Pt−Ru based composites represented the diffraction peaks corresponding to (111), (200), (220), and (311) planes, typical character of a Pt in face-centered cubic (fcc) phase. The diffraction peaks of Pt−Ru nanoparticles in Pt−Ru/STA-C, Pt−Ru/C, and commercial Pt−Ru/C (Johnson Matthey), shifted to higher angles with respect to the diffraction lines of Pt/C (Figure 6a), reflecting the lattice contraction due to the partial substitution of Pt by Ru. The diffraction peaks of the composites Pt/C and Pt−Ru/C produced by hydrogen reduction method were observed to be sharp (panels a and c of Figure 6). On the contrary, very broad peaks were observed for STA containing Pt/STA-C, Pt−Ru/STA-C composites (Figure 6b,e) due to the lowering of particle size as evident from the TEM results (panels a and b of Figure 2).

Electrocatalytic Activity of Pt and Pt−Ru Based Composites for Methanol Oxidation. The electrocatalytic activities and stabilities of Pt and Pt−Ru based catalysts prepared by STA reduction method (Pt/STA-C and Pt−Ru/STA-C) and hydrogen reduction method (Pt/C and Pt−Ru/C) were probed by CV. The CVs of Pt and Pt−Ru based composite electrodes are shown in panels A and B of Figure 7, respectively, and the corresponding electrochemical parameters are listed in Table 1. The two oxidation peaks corresponding to oxidation of methanol and intermediates produced during the methanol oxidation are observed for all the composite electrodes. For comparison, the CV obtained for the methanol oxidation by the commercial Pt−Ru/C (J. M) is presented in Figure 7B(ii). The various parameters including onset potential, mass activity (current density at 0.75 V of methanol oxidation from CV per unit Pt loading mass normalized to electrode geometric area), and the ratio of the forward oxidation current peak (i_f) to the reverse current peak (i_b) are shown in Table 1.

TABLE 1: Electrochemical Characteristics of Composite Electrodes for Methanol Oxidation

catalyst	EAS (m^2g^{-1})	onset potential (V)	i_f/i_b	mass activity (mA cm^{-2})
Pt/C	23.3	0.41	0.80	191
Pt/STA-C	33.0	0.31	1.11	370
Pt−Ru/C	17.2	0.30	0.91	204
Pt−Ru/STA-C	25.6	0.24	1.05	503
Pt−Ru/C (J.M)	22.5	0.25	0.95	271

According to the data listed in Table 1. The onset for methanol oxidation on Pt/C (Figure 7A(ii)) was found to be 0.41 V, which is 100 mV more positive than Pt/STA-C (Figure 7A(i)) electrode (0.31 V). The onset of Pt−Ru/C (Figure 7B(iii)) (0.30 V) was 60 mV more positive than the Pt−Ru/STA-C (Figure 7B(i)) electrode (0.24 V). This gives clear evidence for the superior electrocatalytic activity of STA containing composite electrodes for methanol oxidation.

The STA free Pt/C and Pt−Ru/C prepared by hydrogen reduction method displayed very low mass activity. By contrast, the STA containing Pt/STA-C and Pt−Ru/STA-C composites showed high current density for methanol oxidation. The mass activity for methanol oxidation followed the order: Pt−Ru/STA-C > Pt/STA-C > Pt−Ru/C (J.M) > Pt−Ru/C > Pt/C. The mass activity of Pt/STA-C is 48% higher than Pt/C electrode. The Pt−Ru/STA-C composite showed highest mass activity (503 $mAcm^{-2}$) among all the composites, which is 60% higher than that of Pt−Ru/C and 46% higher than that of commercial catalyst Pt−Ru/C (J.M) from that data in Table 1. These indicate that the composites containing STA have higher catalyst utilization for methanol oxidation reaction.

It can also be seen, in Table 1, that the i_f/i_b ratios of Pt/STA-C (1.11) and Pt−Ru/STA-C (1.05) are higher than that of Pt/C (0.80) and Pt−Ru/C (0.91) electrodes. The (i_f/i_b) ratio is an index of the catalyst tolerance to accumulation of carbonaceous species and the catalysts with high (i_f/i_b) ratio effectively remove the poisoning species more effectively from their surface.[35] The high (i_f/i_b) values for STA containing composites suggest that they are more effective in removing CO species than STA free composites prepared by hydrogen reduction method. The enhanced electrochemical activities of STA containing composite electrocatalysts (Pt/STA-C and Pt−Ru/STA-C) toward methanol oxidation can be attributed to small size and high distribution of Pt and Pt−Ru nanoparticles and assistant catalytic effect of STA as discussed below.

The small sized metal nanoparticles would provide high surface to volume ratio and the high dispersion achieved further increases the number of active sites for the substrate (methanol) adsorption. STA is analogous to its parent metal oxide WO_3 organized around silicate heterogroup. Especially the reduced STA is chemically equivalent to tungsten bronzes in the form of colloidal semiconducting quantum dots.[36,37] The tungsten bronzes are electronic and ionic conducting and also can make the dehydrogenation of methanol molecules adsorbed on Pt surface more effective in acidic electrolyte,[38,39] since the spillover of hydrogen onto the surface of hydrogen tungsten bronze can free these Pt sites for further chemisorption of methanol molecules.[40] As a result, a possible spill over effect between Pt nanoparticles and STA similar to the well-known spillover mechanism between Pt and WO_3 may also occur during electrode reactions. In addition, tungstate units from STA in these composites can provide additional −OH groups or radicals capable of facilitating oxidation of passivating intermediates (CO_{ads}) on Pt.[41] STA was utilized as impregnant in polymer proton exchange membrane electrolytes to improve ionic conductivity.[21] The excellent electron transfer ability and high proton conductivity of STA[20] can increase the conductivity of the composite electrode and promote the electron transfer reactions. The strong oxidizing capability of POMs (STA) toward CO can improve the catalyst tolerance toward CO like poisoning species.[42]

To test the tolerance toward poisoning and long-term performance of the Pt and Pt−Ru nanoparticles on the carbon support toward the methanol oxidation reaction, chronoamperometric studies have been performed in 1 M H_2SO_4 solution containing 1 M CH_3OH at constant potential 0.5 V for 3600 s (panels C and D of Figure 7). Inspite of the initial high current density, there is a constant decay in the current with respect to time for Pt/C (Figure 7C(ii)) and Pt−Ru/C (Figure 7D(iii)) electrodes respectively and it reached the minimum during the period of study. This indicates that these electrodes decay faster due to poisoning. On the other hand, for the STA containing electrodes, Pt/STA-C (Figure 7C(i)) and Pt−Ru/STA-C (Figure 7D(i)), the rate of current decay is small and achieved a steady state current at long times. The long-term performance of STA containing electrodes is comparable to that of the commercial catalyst (Figure 7D(ii)), suggesting high tolerance toward poisoning. These better electrocatalytic activity and greatly reduced effect of CO poisoning suggest that STA containing composites Pt/STA-C and Pt−Ru/STA-C are promising anode electrocatalysts for direct methanol fuel cells.

Conclusions

In summary, well dispersed Pt and Pt−Ru nanoparticles on carbon were synthesized by utilizing the facile electron transfer and reducing capabilities of STA. The designed composite electrode materials containing STA were tested for electrochemical energy conversion and storage application. The application of Pt/STA-C and Pt−Ru/STA-C composites as anode electrocatalysts was initially investigated. It was found that these composites exhibit higher catalytic activity and stability for electrochemical methanol oxidation than STA free Pt/C and Pt−Ru/C as well as commercial Johnson Matthey Pt−Ru/C catalysts. This study is of great significance in the development of efficient electrocatalysts for direct methanol fuel cells.

Acknowledgment. This work was supported by the Council for Scientific and Industrial Research (CSIR), New Delhi, India.

Supporting Information Available: EDX patterns of Pt/STA-C, Pt−Ru/STA-C, and Ru/STA-C. SEM and EDX mapping of Pt/STA-C. This material is available free of charge via the Internet at http://pubs.acs.org.

References and Notes

(1) Winter, M.; Brodd, R. J. *Chem. Rev.* **2004**, *104*, 4245.
(2) Bergamaski, K.; Pinheiro, A. L. N.; Neto, E. T.; Nart, F. C. *J. Phys. Chem. B* **2006**, *110*, 19271.
(3) Liu, Z.; Ling, X. Y.; Su, X.; Lee, J. Y. *J. Phys. Chem. B* **2004**, *108*, 8234.
(4) Su, F.; Zeng, J.; Zao, X.; Yu, Y.; Lee, J. Y.; Zhao, X. S. *Chem. Mater.* **2005**, *17*, 3960.
(5) Kongkanand, A.; Kuwabata, S.; Girishkumar, G.; Kamat, P. *Langmuir* **2006**, *22*, 2392.
(6) Kunimatsu, K.; Shimazu, K.; Kita, H. *J. Electroanal. Chem.* **1988**, *256*, 371.
(7) Hogarth, M.; Hards, G. *Platinum Met. Rev.* **1996**, *40*, 150.
(8) Beden, B.; Lamy, C.; Bewick, A.; Kunimatsu, K. *J. Electroanal. Chem.* **1981**, *121*, 343.
(9) Lu, C.; Masel, R. I. *J. Phys. Chem. B* **2001**, *105*, 9793.
(10) Frelink, T.; Visscher, W.; Vanveen, J. A. R. *Surf. Sci.* **1995**, *335*, 353.
(11) Tong, Y. Y.; Kim, H. S.; Babu, P. K.; Waszczuk, P.; Wieckowski, A.; Oldfield, E. *J. Am. Chem. Soc.* **2002**, *124*, 468.
(12) Watanabe, M.; Motoo, S. *J. Electroanal. Chem.* **1975**, *60*, 267.
(13) Yajima, T.; Wakabayashi, N.; Uchida, H.; Watanabe, M. *Chem. Commun.* **2003**, 828.
(14) Tian, J.; Sun, G.; Jiang, L.; Yan, S.; Mao, Q.; Xin, Q. *Electrochem. Commun.* **2007**, *9*, 563.
(15) Hepel, M.; Kumarihamy, I.; Zhong, C. J. *Electrochem. Commun.* **2006**, *8*, 1439.
(16) Ke, K.; Waki, K. *J. Electrochem. Soc.* **2007**, *154*, A207.
(17) Maiyalagan, T.; Viswanathan, B.; Varadaraju, U. V. *J. Nanoscience. Nanotech.* **2006**, *6*, 2067.
(18) Rajeswari, J.; Viswanathan, B.; Varadarajan, T. K. *Mater. Chem. Phys.* **2007**, *106*, 168.
(19) Pope, M. T. *Heteropoly and Isopoly Oxometalates*; Springer-Verlag: Berlin, 1983.
(20) Tian, H.; Savadogo, O. *Fuel Cells* **2005**, *5*, 375.
(21) Helen, M.; Viswanathan, B.; Murthy, S. S. *J. Membr. Sci.* **2007**, *292*, 98.
(22) Horky, A.; Kherani, N. P.; Xu, G. *J. Electrochem. Soc.* **2003**, *150*, A1219.

(23) Verga, M.; Papaconstantinou, E.; Pope, M. T. *Inorg. Chem.* **1970**, *9*, 662.
(24) Chan, K. Y.; Ding, J.; Ren, J.; Cheng, S.; Tsang, K. Y. *J. Mater. Chem.* **2004**, *14*, 505.
(25) Kogan, V.; Aizenshtat, Z.; Biro, R. P.; Neumann, R. *Org. Lett.* **2002**, *4*, 3529.
(26) Troupis, A.; Hiskia, A.; Papaconstantinou, E. *Angew. Chem., Int. Ed.* **2002**, *41*, 1911.
(27) Ge, M.; Zhong, B.; Klemperer, W. G.; Gewirth, P. *J. Am. Chem. Soc.* **1996**, *118*, 5812.
(28) Kulesza, P. J.; Chojak, M.; Karnicka, K.; Miecznikowski, K.; Palys, B.; Lewera, A.; Wieckowski, A. *Chem. Mater.* **2004**, *16*, 4128.
(29) Garrigue, P.; Delville, M. H.; Labrugere, C.; Cloutet, E.; Kulesza, P. J.; Morand, J. P.; Kuhn, A. *Chem. Mater.* **2004**, *16*, 2984.
(30) Kang, Z.; Wang, E.; Mao, B.; Su, Z.; Gao, L.; Lian, S.; Xu, L. *J. Am. Chem. Soc.* **2005**, *127*, 6534.
(31) Rohlfing, F.; Kuhn, A. *Carbon* **2006**, *44*, 1942.
(32) Deitcheff, C. R.; Fournier, M.; Franck, R.; Thovenot, R. *Inorg. Chem.* **1983**, *22*, 207.
(33) Gullon, J. S.; Iglesias, F. V.; Montiel, V.; Aldez, A. *Electrochim. Acta* **2004**, *49*, 5079.
(34) Chu, D.; Gilman, S. *J. Electrochem. Soc.* **1996**, *143*, 1685.
(35) Mu, Y.; Liang, H.; Hu, J.; Jiang, L.; Wan, L. *J. Phys. Chem. B* **2005**, *109*, 22212.
(36) Romero, P. G.; Pastor, N. C. *J. Phys. Chem.* **1996**, *100*, 12448.
(37) Romero, P. G. *Solid State Ionics* **1997**, *101*, 243.
(38) Tseung, A. C. C.; Chen, K. Y. *Catal. Today.* **1997**, *38*, 439.
(39) Shen, P. K.; Tseung, A. C. C. *J. Electrochem. Soc.* **1994**, *141*, 3082.
(40) Hobbs, B. S.; Tseung, A. C. C. *Nature* **1969**, *222*, 556.
(41) Shen, P. K.; Chen, K. Y.; Tseung, A. C. C. *J. Electrochem. Soc.* **1995**, *142*, L85.
(42) Kim, W. B.; Voitl, T.; Rodriguez, G. J.; Dumesic, J. A. *Science* **2004**, *305*, 1280.

JP8100514